AGU PUBLICATIONS

JGR

Journal of Geophysical Research: Biogeosciences

RESEARCH ARTICLE

10.1002/2016JG003725

Key Points:
- Observations from SPRUCE conditioned TECO model which forecasted soil thermal dynamics under future warming
- Air warming caused stronger soil warming in summer than winter and dramatic reduction in snow depths
- Uncertainty is smaller for forecasting soil temperature but large for snow and frozen depths

Supporting Information:
- Supporting Information S1
- Data Set S1
- Data Set S2

Correspondence to:
Y. Huang,
yuanyuanhuang2011@gmail.com

Citation:
Huang, Y., J. Jiang, S. Ma, D. Ricciuto, P. J. Hanson, and Y. Luo (2017), Soil thermal dynamics, snow cover, and frozen depth under five temperature treatments in an ombrotrophic bog: Constrained forecast with data assimilation, *J. Geophys. Res. Biogeosci.*, *122*, 2046–2063, doi:10.1002/2016JG003725.

Received 21 NOV 2016
Accepted 28 JUL 2017
Accepted article online 7 AUG 2017
Published online 18 AUG 2017

Soil thermal dynamics, snow cover, and frozen depth under five temperature treatments in an ombrotrophic bog: Constrained forecast with data assimilation

Yuanyuan Huang[1], Jiang Jiang[1,2], Shuang Ma[1], Daniel Ricciuto[3], Paul J. Hanson[3], and Yiqi Luo[1,4]

[1]Department of Microbiology and Plant Biology, University of Oklahoma, Norman, Oklahoma, USA, [2]Key Laboratory of Soil and Water Conservation and Ecological Restoration in Jiangsu Province, Collaborative Innovation Center of Sustainable Forestry in Southern China of Jiangsu Province, Nanjing Forestry University, Nanjing, China, [3]Environmental Sciences Division and Climate Change Science Institute, Oak Ridge National Laboratory, Oak Ridge, Tennessee, USA, [4]Department of Earth System Science, Tsinghua University, Beijing, China

Abstract Accurate simulation of soil thermal dynamics is essential for realistic prediction of soil biogeochemical responses to climate change. To facilitate ecological forecasting at the Spruce and Peatland Responses Under Climatic and Environmental change site, we incorporated a soil temperature module into a Terrestrial ECOsystem (TECO) model by accounting for surface energy budget, snow dynamics, and heat transfer among soil layers and during freeze-thaw events. We conditioned TECO with detailed soil temperature and snow depth observations through data assimilation before the model was used for forecasting. The constrained model reproduced variations in observed temperature from different soil layers, the magnitude of snow depth, the timing of snowfall and snowmelt, and the range of frozen depth. The conditioned TECO forecasted probabilistic distributions of soil temperature dynamics in six soil layers, snow, and frozen depths under temperature treatments of +0.0, +2.25, +4.5, +6.75, and +9.0°C. Air warming caused stronger elevation in soil temperature during summer than winter due to winter snow and ice. And soil temperature increased more in shallow soil layers in summer in response to air warming. Whole ecosystem warming (peat + air warmings) generally reduced snow and frozen depths. The accuracy of forecasted snow and frozen depths relied on the precision of weather forcing. Uncertainty is smaller for forecasting soil temperature but large for snow and frozen depths. Timely and effective soil thermal forecast, constrained through data assimilation that combines process-based understanding and detailed observations, provides boundary conditions for better predictions of future biogeochemical cycles.

1. Introduction

Soil temperature is a key regulator of numerous biophysical and biogeochemical processes. Soil temperature has been shown to strongly affect gases exchange [*Li et al*., 2000; *Elberling et al*., 2008], soil hydrological dynamics [*Hopmans and Dane*, 1986], soil organic matter (SOM) decomposition [*Melillo et al*., 2002; *Davidson and Janssens*, 2006; *Allison et al*., 2010], plant nutrient uptake [*Melillo et al*., 2002], and growing season length [*Euskirchen et al*., 2006]. Among various processes affected by soil temperature, SOM decomposition is especially important for understanding the carbon cycle-climate change feedback as soil stores the largest portion of organic carbon in terrestrial ecosystems [*Ciais et al*., 2013; *Luo et al*., 2016]. However, large uncertainties still remain on SOM dynamics despite decades of studies. For example, *Todd-Brown et al*. [2013] pointed out a large range of contemporary soil carbon storage (510–3040 Gt C) reported by 11 Earth system models. As a result, projected soil organic carbon change ranges from a loss of 72 Gt C to a gain of 253 Gt C over the 21st century (2090–2099 minus 1997–2006) among these 11 Earth system models [*Todd-Brown et al*., 2014]. The large uncertainties in modeled SOM are at least partly due to variations in soil environmental conditions among the models [*Betts and Ball*, 1997; *Verry et al*., 2011; *Luo et al*., 2016]. Thus, accurately simulating soil environmental variables, such as temperature, is essential for better predicting of future terrestrial carbon cycling [*Luo et al*., 2016].

Air temperature is one of the main drivers of soil temperature [*Farouki*, 1981; *DeGaetano et al*., 1996; *Peng et al*., 2016]. Therefore, soil temperature is frequently extracted from air temperature based on the empirical relationship between air and soil temperatures [*Toy et al*., 1978; *Zhang*, 2005; *Mackiewicz*, 2012], leaving the

real soil temperature less well known compared to air temperature. Snow cover provides an effective insulating barrier, decoupling the soil thermal dynamics from localized air temperatures especially during winter in northern ecosystems [*Zhang*, 2005; *Schaefer et al*., 2009; *Ge and Gong*, 2010]. The insulation impact of snow is evident from the lagged or asymmetric response of soil temperature to changing meteorological conditions [*Mackiewicz*, 2012]. For example, *Park et al*. [2014] reported a stronger warming rate of soil temperature compared to air temperature in Russia over 1921–2011 with the potential contribution from snow depth. Snow cover also alters surface energy balance response due to surface albedo change and to a smaller extent, the insulating effects of snow cover on diffusive heat fluxes and the latent heat flux from snowmelt [*Pomeroy and Brun*, 2001; *Ge and Gong*, 2010]. Soil freeze and thaw events can temporarily alter soil temperature by releasing and absorbing large amount of latent heat [*Williams and Smith*, 1989]. And explicit incorporation of heat exchanges during soil freeze-thaw cycles is reported to improve the simulation of soil temperatures and its variability at seasonal and interannual scales [*Luo et al*., 2003].

In regions such as the northern peatland and permafrost where snow and ice play an important role, soil carbon density is high but potentially vulnerable to soil temperature changes [*Granberg et al*., 1999; *Roulet et al*., 2007; *Koven et al*., 2011; *Ciais et al*., 2013; *Schuur et al*., 2015; *Hanson et al*., 2016a]. Future climate warming is expected to enhance the decomposition of SOM from thawing permafrost and/or drying and aerating peatlands, which is expected to trigger a positive feedback to climate warming through releasing of greenhouse gases such as CO_2 and CH_4 [*Koven et al*., 2011; *Tfaily et al*., 2014; *Schuur et al*., 2015; *Hanson et al*., 2016a]. The magnitude of such feedback depends partially on the temperature sensitivity of SOM decomposition and partially on the degree of soil temperature change. There are, however, large discrepancies in current prediction of soil temperature dynamics in these ecosystems [*Koven et al*., 2013; *Peng et al*., 2016], which limit our understanding of how such ecosystems will respond and feedback to future climate change. *Koven et al*. [2013] revealed that current disagreement in modeled mean soil temperatures from the Coupled Model Intercomparison Project phase 5 (CMIP5) in permafrost region is mediated mainly by snow in winter. And accurate prediction of snow impacted soil temperature dynamics is therefore an important step forward for understanding the carbon response in these vulnerable ecosystems.

Realistic prediction of soil temperature dynamics relies on models that combine our current best knowledge related to processes or mechanisms that govern soil temperature dynamics. Prediction becomes more effective when models are timely informed by observations through techniques such as data assimilation [*Luo et al*., 2011]. Numerical weather forecasting is the classic example that benefits from constantly updating process-based models through assimilation of observations [*Kalnay*, 2002]. Similarly, when the process-based modeling of soil temperature is trained by observations through data assimilation, the prediction accuracy of soil temperature is expected to be improved since data assimilation techniques aim to minimize the difference between observations and mechanistic understanding of soil temperature dynamics [*Xu et al*., 2006; *Luo et al*., 2011]. In addition, data assimilation such as Markov Chain Monte Carlo method allows for the estimation of model uncertainty [*Gelman and Rubin*, 1992; *Xu et al*., 2006], which is useful in providing probabilistic information on forecasting. However, current process-oriented modeling of soil thermal dynamics has not taken full advantage of data assimilation techniques. Most of the modeling studies fix or tune model parameters without quantification of uncertainty [*Zhang et al*., 2003; *Zhang et al*., 2008; *Schaefer et al*., 2009; *Jungqvist et al*., 2014]. In this study, we integrated process-based understanding of soil thermal dynamics (including the snow cover and the freeze-thaw cycle) with data through data assimilation to obtain better probabilistic predictions of future soil thermal dynamics which will be beneficial for predicting terrestrial biogeochemical cycles.

2. Methods

2.1. SPRUCE Project and Site Description

We took the Spruce and Peatland Responses Under Climatic and Environmental change (SPRUCE) experiment as our case study. SPRUCE is a project designed to study the response of northern peatland to climate warming and elevated atmospheric CO_2 concentration [*Hanson et al*., 2016c] with long-term whole ecosystem manipulations (planned for 10 years). SPRUCE site is located in the U.S. Department of Agriculture (USDA) Forest Service Marcell Experimental Forest (MEF, 47°30.476′N, 93°27.162′W) in northern Minnesota [*Kolka et al*., 2011]. MEF is a temperate bog forest located at the southern end of boreal forest with rapid

diurnal and seasonal temperature fluctuations, which is vulnerable to climate change and also plays an important role in feeding back to future climate change with its large storage of SOM [*Hanson et al*., 2016c]. The mean annual precipitation is 780 mm. And the mean annual temperature is 3.3°C with daily mean minimum and maximum of −38°C and 30°C, respectively. Approximately two thirds of precipitation occurs as rainfall and the remaining as snowfall. Mean annual air temperatures have increased ~0.4°C per decade over the last 40 years [*Sebestyen et al*., 2011]. In this study, we focus mainly on the S1-bog, a *Picea-Sphagnum* bog where the pretreatment measurements were collected. The S1-bog is part of the USDA Forest Service Northern Research Station that has been studied for more than 50 years. Vegetation within the S1-bog is dominated by *Sphagnum sp*. moss and tree species *Picea mariana* and *Larix laricina*. Peat depth in this area is around 2–4 m with a maximum depth of 11 m [*Tfaily et al*., 2014; *Shi et al*., 2015; *Hanson et al*., 2016c]. Soil in this studying site is composed primarily of organic matter, with a total porosity of 84%–97% [*Verry et al*., 2011]. And the water table generally fluctuates within the top 30 cm [*Sebestyen et al*., 2011; *Shi et al*., 2015].

Although SPRUCE experiments focus on ecosystem's response to temperature and CO_2 manipulations, the pretreatment data collected from SPRUCE (January 2010 to December 2014 for this study) includes environmental variables such as climatic forcing, snow depth (half hourly), soil temperatures (half hourly) at different layers, water table, and sparsely frozen depth. These pretreatment data provide valuable information to develop and test the soil temperature model [*Krassovski et al*., 2015]. The half hourly environmental monitoring data [*Hanson et al*., 2011] that are used to drive the TECO model were averaged to an hourly time step to match model simulations for this study. Measurements obtained since the warming treatment period (2015–2016) served to validate the general pattern of model forecast. Briefly, the climatic forcing, water table, and snow depth were monitored at the meteorological station EM1 approximately 3 m away from S1-bog. Climatic forcing were generally recorded 2 m above the surface. Water table was monitored through water level sensors and recorded through dataloggers [*Shi et al*., 2015]. Soil temperature has been monitored at one unchambered plot at different soil depths based on which the soil module was configured. Meanwhile, chambered plots were set up to manipulate temperature and atmospheric CO_2 concentration since year 2014. Detailed information about the warming treatments is available in section 2.5 and currently available observations are described in *Hanson et al*. [2016c]. Relevant measurements were obtained from the SPRUCE webpage (http://mnspruce.ornl.gov/), the archived ftp site (ftp://sprucedata.ornl.gov), or the specific location as indicated in citations from following sections.

2.2. Model Description

2.2.1. General Overview

Terrestrial ECOsystem (TECO) model is a process-based ecosystem model that couples terrestrial carbon, nitrogen, and water cycles. The original TECO model has four major submodules: canopy, soil water, vegetation dynamics, and soil carbon/nitrogen. Detailed description of TECO is available in *Weng and Luo* [2008] and *Shi et al*. [2016].

Canopy photosynthesis that couples surface energy, water, and carbon fluxes is based on a two-big-leaf model [*Wang and Leuning*, 1998]. Leaf photosynthesis and stomatal conductance are similar as in *Farquhar et al*. [1980] and *Ball et al*. [1987], respectively. Transpiration and associated latent heat losses are controlled by stomatal conductance, soil moisture, and rooting pattern. Soil moisture content in different soil layers is regulated by water inputs (precipitation and percolation) and outputs (transpiration, evaporation, and runoff). Evaporation losses of water and associated latent heat are regulated by moisture content in the first soil layer and atmospheric demand. Vegetation dynamic module takes into account vegetation growth, carbon allocation, and phenology. Soil carbon/nitrogen module tracks carbon and nitrogen through processes such as litterfall, SOM decomposition, and mineralization. Vegetation and soil carbon/nitrogen dynamics indirectly affect surface energy partition that might impact soil thermal dynamics, such as through the amount of leaf that performs photosynthesis and the transpiration strength.

TECO has been adapted to the SPRUCE site to study the carbon dynamics (by Jiang Jiang and Shuang Ma). As the SPRUCE site is characterized by frequent water-logged periods (i.e., water table is above the ground), soil hydrology was slightly modified by allowing water to accumulate above the ground. Meanwhile, a fraction of the standing water ($r_{percent}$) is lost to mimic the runoff and lateral water flowing out of the system. A diagnostic water table module was added to TECO following *Granberg et al*. [1999]. As the observed historical water

table rarely went below 30 cm belowground [*Sebestyen et al*., 2011; *Shi et al*., 2015], water table depth is therefore diagnosed from water content above that 30 cm peat profile (including the standing water). Key parameters that regulate carbon dynamics, for example, the maximum rate of carboxylation (V_{cmax}), specific leaf area (SLA), and turnover rates of different carbon pools, were constrained through assimilation of carbon-related observations. The documentation of the constrained model that is suitable for SPRUCE is available from the github repository (https://github.com/ou-ecolab), and the model performance is displayed through the Ecological Platform for Assimilation of Data into models (EcoPAD) (http://ecolab.cybercommons.org/ecopad_portal/).

In studies mentioned above, soil temperature was treated as an input. We further improved the original TECO model by incorporating snow dynamics and explicitly tracking heat transfers between different soil layers and during the freeze-thaw cycle. We followed the original TECO structure by dividing soil into 10 layers. The thickness for each soil layer is 5 cm, 15 cm, 20 cm, 40 cm, 80 cm, 40 cm, 40 cm, 40 cm, 40 cm, and 40 cm. The first six layers are in line with depths at which observations were reported, and the last four layers were set up to give a total depth of 3.6 m to reflect the typical depth of the peat profile in the studying area. The model requires climate variables such as air temperature, relative humidity, vapor pressure deficit, rainfall, wind speed, photosynthetically active radiation, and shortwave and longwave radiations and predicts soil temperature, snow mass in water equivalent, snow depth, and frozen depth.

2.2.2. Surface Energy Budget and Boundary Temperature

Surface energy budget (W m^{-2}) is taken largely from the original model that simulates net radiation (longwave (L) and shortwave (S)), latent heat (λE), sensible heat (H), and ground heat (G). The net radiation goes through a radiation submodule which tracks photosynthetically active radiation (PAR), near infrared radiation, and thermal radiation from interactions between the atmosphere, sunlit and shaded leaves, and the soil surface [*Wang and Leuning*, 1998; *Weng and Luo*, 2008]. Latent heat loss is associated with loss of water through evaportranspiration. Sensible heat is proportional to the temperature difference between soil surface and air. Ground heat flux is related to temperature difference between soil surface and the top soil layer. Soil surface temperature is derived from surface energy balance similar as in the thermal model from *Luo et al*. [1992] and is used as the upper boundary condition for heat transfers within snow and soil layers.

$$f(T_0) = (1-\alpha)S\downarrow + (L\uparrow - L\downarrow) + H + \lambda E + G \tag{1}$$

where T_0 is the soil surface temperature and α is albedo. We differentiate the surface albedo during nonsnow covered and snow covered period. The function $f(T_0)$ and derivation of T_0 is available from *Luo et al*. [1992].

2.2.3. Snow Dynamics

Snow cover increases surface albedo which reduces the net radiation at the surface. Meanwhile, the insulation effect of snow acts to prevent heat loss from soil during winter.

A simple one layer snow model at a daily time step is applied in this study and the snow module takes into account the insulation and albedo effects. Currently, the snow dynamics are directly driven by climatic forcing with an empirical factor (as a parameter) taking into account the vegetation impact and can be run independently from the original TECO model. Snow mass dynamics in water equivalent is based on the mass balance. And snow depth (h_{snow}) is linked to snow mass through snow density (ρ_{snow}).

$$\frac{dM_{snow}}{dt} = I_s - S - M \tag{2}$$

$$h_{snow} = \frac{M_{snow}}{\rho_{snow}} \tag{3}$$

where M_{snow} is snow mass in water equivalent (in units of mm or kg/m^2), I_s is snowfall rate, S is snow sublimation rate, and M is snow melting rate.

A threshold of 0°C in daily air temperature is applied to partition daily precipitation into either rainfall or snowfall. Sublimation of snow is controlled by a function [*Rawlins et al*., 2003] which takes into account air temperature below freezing, daylength and saturated vapor pressure,

$$S = f_{sub} \times D \times \frac{e_{sat}(T_a)}{T_a + 273.2} \tag{4}$$

where f_{sub} is an empirical factor, D is the fraction of the day (daylength), and $e_{sat}(T_a)$ is daily saturated vapor pressure at T_a (°C).

Snowmelt is a function of rainfall, air temperature, and snow age (in days), and currently, the snow module does not take into account the feedback of soil temperature on snow melting,

$$M = f_v \times (2.63 + 2.55 \times T_a + 0.0912 \times T_a \times P_t) \times e^{-m \times d/365} \quad (5)$$

where f_v (dimensionless) is a vegetation factor which reflects the impact of vegetation cover on snow melting. P_t (mm d^{-1}) is daily precipitation. d is snow age in days, and m is an empirical factor regulates the impact of snow age on melting rate.

2.2.4. Soil Temperature

Temperature dynamics within snow and soil layers are based on the equation where the change of temperature over time ($\frac{\partial T}{\partial t}$) is proportional to the difference in heat influx and efflux. Heat fluxes (influx or efflux) equal to soil thermal conductivity (k, W m^{-1} K^{-1}) times the temperature gradient ($\frac{\partial T}{\partial z}$, K m^{-1}),

$$c\frac{\partial T}{\partial t} = \frac{\partial}{\partial z}\left(k\frac{\partial T}{\partial z}\right) \quad (6)$$

where c is heat capacity (J m^{-3} K^{-1}). We treat snow as a single layer box which may vary in depth. To represent the impact of snow depth on the insulation effect [*Pomeroy and Brun*, 2001; *Ge and Gong*, 2010], we incorporate a depth related regulator f_d which indicates stronger insulation effect with deeper snow cover,

$$f_d = e^{(-a \times h)} \quad (7)$$

where a is an insulation factor and h is snow depth in centimeters.

Soil thermal conductivity and heat capacity in each soil layer i are the weighted averages among different soil components, where the weights correspond to the volume fraction of each component,

$$c_i = w_{liq,i}c_{water} + w_{ice,i}c_{ice} + (1 - \theta_{sat})c_{soil} + (\theta_{sat} - w_{liq,i} - w_{ice,i})c_{air} \quad (8)$$

$$k_i = w_{liq,i}k_{water} + w_{ice,i}k_{ice} + (1 - \theta_{sat})k_{soil} + (\theta_{sat} - w_{liq,i} - w_{ice,i})k_{air} \quad (9)$$

where c_{water}, c_{ice}, c_{soil}, c_{air} are the heat capacity of water, ice, soil and air, respectively, and k_{water}, k_{ice}, k_{soil}, k_{air} are the corresponding thermal conductivity for each component. $w_{liq,i}$ is the liquid water content in each soil layer, $w_{ice,i}$ is the volumetric ice content for each soil layer, and θ_{sat} is the saturated soil water content. The soil in this study site is formed primarily by organic matter with little mineral components. C_{soil} and k_{soil} are therefore set up to reflect the thermal properties of organic matter [*Lawrence and Slater*, 2008] which are relatively constant. Thermal properties of water, ice, and air are physical constants. We left the boundary (between the atmosphere and soil surface) heat conductivity as a free parameter to be constrained by observations, and boundary heat capacity is treated the same as that in the first soil layer.

Phase change of water absorbs or releases a large amount of heat. The critical point of freeze-thaw transition is set at 0°C; that is, when soil temperature drops below 0°C, available soil water turns into ice and releases energy into soil and *vice versa*. The amount of heat released during freeze or the heat absorbed to thaw the ice equals to the latent heat of fusion (L_f) times the amount of soil water/ice involved in the transition.

2.3. Data Assimilation

Markov Chain Monte Carlo (MCMC) method is used to estimate the distribution of model parameters [*Xu et al*., 2006]. MCMC is based on Bayesian statistics in which the posterior distribution $p(\theta|O)$ of model parameters θ for given observations O is proportional to the likelihood function $p(O|\theta)$ and the prior distribution $p(\theta)$.

$$p(\theta|O) \propto p(O|\theta)p(\theta) \quad (10)$$

Here we assume the prior distribution is in uniform and within the range obtained from literature or empirical knowledge. We also assume errors between observation and model simulation follow Gaussian distribution with zero means. Therefore, the likelihood function takes the following form,

Table 1. Parameters Involved in Data Assimilation

	Range	Unit	Long Name	Reference
c_{snow}	[20,909, 1,150,000]	J m^{-3} K^{-1}	Heat capacity of snow	*Pomeroy and Brun* [2001]
k_{snow}	[0.01, 0.56]	W m^{-1} K^{-1}	Heat conductivity of snow	*Pomeroy and Brun* [2001]
$k_{boudary}$	[0.023, 0.23]	W m^{-1} K^{-1}	Heat conductivity of the upper boundary layer	*Williams and Smith* [1989]
a	[0, 0.1]		Insulation factor	
w_{smax}	[0.85, 0.98]		Total porosity	*Granberg et al.* [1999] and *Verry et al.* [2011]
$r_{percent}$	[0.0001, 0.02]		Fraction of water leaves the system as runoff	*Weng and Luo* [2008]
α	[0.06, 0.2]		Albedo	*Betts and Ball* [1997]
fv	[0.1, 1]		Vegetation factor on snow melting	and *Rawlins et al.* [2003]
f_{sub}	[0.1, 1]		Empirical factor affects snow sublimation rate	*Rawlins et al.* [2003]
ρ_{snow}	[50, 500]	kg m^{-3}	Snow density	*Pomeroy and Brun* [2001]
m	[0.1, 10]		Aging factor on snow melting	*Rawlins et al.* [2003]

$$p(O|\theta) \propto \exp\left\{-\sum_{i=1}^{8}\sum_{t\in O_i}\frac{[O_i(t)-X(t)]^2}{2\sigma_i^2(t)}\right\} \tag{11}$$

where $O_i(t)$ is the ith (a total of 8 in this study, soil temperatures from six layers, snow depth and water table) observation set at time t, $X(t)$ is the simulated corresponding variable, and $\sigma_i(t)$ is the standard deviation of each observation set.

The posterior distribution of parameters were sampled through MCMC with the adaptive Metropolis-Hastings (M-H) algorithm. We repeatedly proposed a new vector of candidate parameters based on the accepted parameters in the previous step by a proposal distribution. The new set of candidate parameters was accepted if it reduced the model observation error or otherwise randomly with a probability of 0.05. More details on sampling posterior distribution is available in [*Xu et al*., 2006]. We tested five chains (each with 50,000 simulations) and used the Gelman-Rubin statistic [*Gelman and Rubin*, 1992] to check the convergence of these chains. From *Gelman et al*. [2003] and previous tests in TECO [*Xu et al*., 2006], five chains are sufficient for convergence tests. We used only the second half of these accepted parameters for posterior analysis, while the first half was taken as in a burn-in period which is sufficient in this study.

We first selected eight parameters that directly regulate snow and soil temperature dynamics for data assimilation. They are snow conductivity (k_{snow}), snow heat capacity (c_{snow}), surface boundary layer conductivity ($k_{boudary}$), insulation factor (a), vegetation factor on snow melting (f_v), an empirical factor on snow sublimation rate (f_{sub}), snow density (ρ_{snow}), and the aging factor on snow melting rate (m). In addition, we selected three parameters that control soil hydrology and surface energy status which may have important indirect consequences on soil thermal dynamics. They are total peat porosity, i.e., the saturated soil water content (Θ_{sat}), the fraction of standing water lost as runoff or lateral flows ($r_{percent}$), and the nonsnow covered surface albedo (α). Detailed information on these parameters is available in Table 1. Parameter ranges in Table 1 were determined through combining information from literature, previous tests of the model and accumulated knowledge about the studying site. Soil temperature and snow depth measured during the pretreatment stage (2011–2014) were used as observations to constrain model parameters.

2.4. Stochastic Weather Generation and Forecasting

Air temperature and precipitation directly affect snow dynamics. We generated 300 sets of 10 year climate forcing (2015–2024). Daily air temperature and precipitation were stochastically generated based on historical data (1961–2014) from the USDA MEF station using a vector autoregressive model (Figure 1).

To match the model time step, hourly temperature was interpolated from daily maximum and minimum, while hourly precipitation was obtained from evenly distributing daily precipitation for each hour. The rest of forcing variables were randomly drawn from frequency distributions at a given hour of each month based on historical observations. Specifically for air temperature, the generated temperature generally follows the same distribution as the historical temperature (Figure 1a). The standard deviation of generated temperature decreases with increasing daily mean temperature (Figure 1c). Therefore, the uncertainty of generated future temperature is larger in winter compared to summer. Stochastically generated future precipitation is similar to the historical precipitation with a slightly higher variation (Figures 1b and 1d).

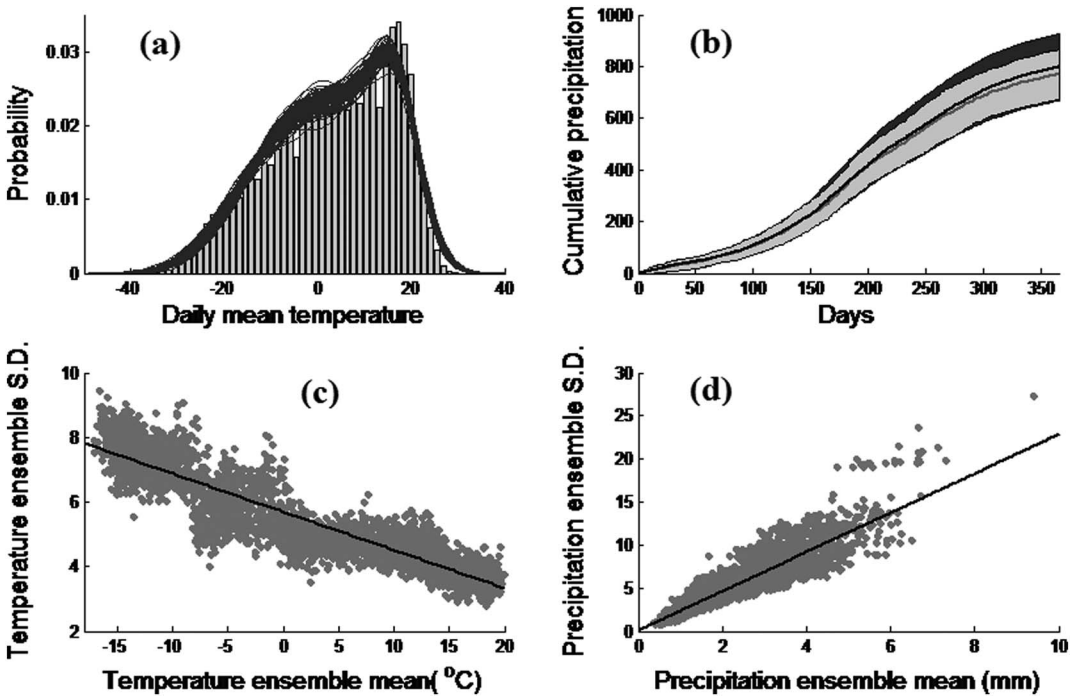

Figure 1. Characteristic of historical and future stochastically generated air temperature and precipitation. (a) Probability distribution of daily mean temperature. Gray bars represent historical observations (1961–2014), and black curves represent the ensemble of generated future temperatures. (b) Cumulative precipitation within a year. Curve and shaded areas represent mean and standard deviation, respectively. Gray is historical observations, and black is the generated future predictions. (c and d) Standard deviations versus means for daily air temperature and precipitation, respectively. Credits from Jiang Jiang.

With stochastically generated weather variables, we conducted 100 forecasting runs by randomly choosing climate forcing or/and parameter sets from their posterior distributions.

2.5. Warming Treatment

In SPRUCE field manipulations, warming treatments include ambient (+ 0.0°C), +2.25°C, +4.5°C, +6.75°C and +9°C. The field warming treatments heat both the deep peat and the air (i.e., whole ecosystem warming). The whole ecosystem warming was achieved through two steps: the first step was achieved by sustaining the deep peat warming since June 2014, and in the second step, the air warming was turned on starting from August 2015 [*Hanson et al*., 2016c]. The manipulative field soil warming is sustained through automatically adding heat into the system when soil temperature falls below the target, while the air warming is realized through modified open-top chambers (115 m^2). The whole ecosystem warming is unique in its up to 3 m deep peat heating and the inclusion of tall trees in the air warming chambers. The goal of the field manipulations is to provide a plausible ecosystem warming conditions with a regression-based experimental design to study responses of biological activities and ecosystem functions. In addition to warming, the manipulations also have elevated CO_2 treatments. Warming plots were selected to minimize background differences and each treatment was not accompanied by replicates. So there are 10 chambers in total (5 with warming treatments and 5 with both warming and elevated CO_2 treatments) [*Hanson et al*., 2016c]. In this study, we focus mainly on the warming-only responses.

As the manipulative field warming measurements are ongoing and associated environmental data are not readily available at this stage, we do not aim to reproduce the exact chambered conditions for each treatment. The enclosure by chambers is likely to alter the climatic conditions. As a first step, we explore the plausible thermal responses to warming treatments through imposing warming treatments under information obtained from nonchambered conditions assuming the alterations in climatic conditions caused by chambers are the same for each warming treatment. In this way, we aim to reveal a general response pattern instead of the exact response value. We mimicked SPRUCE warming treatments by increasing soil

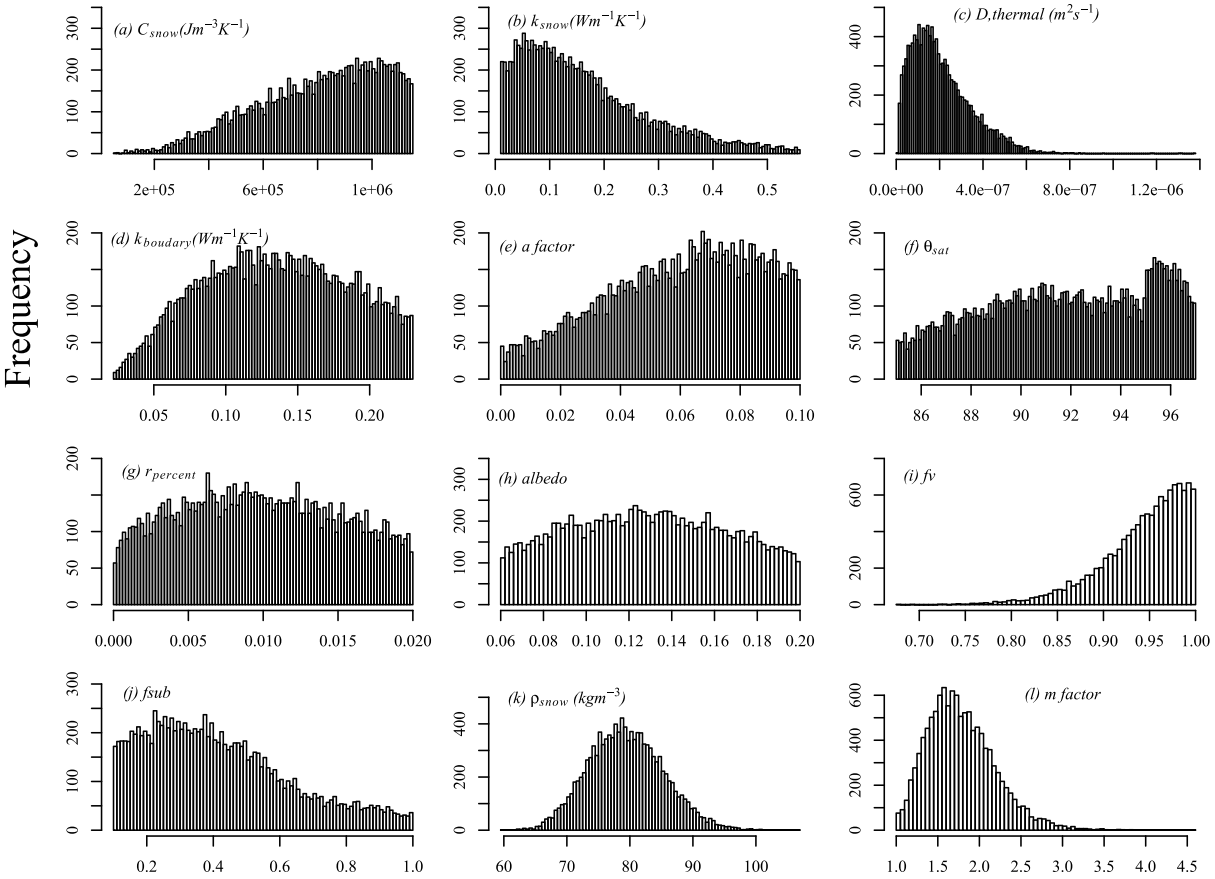

Figure 2. Posterior distributions of parameters involved in data assimilation. (a) Heat capacity of snow; (b) heat conductivity of snow; and (c) diffusivity of snow, i.e., the ratio between heat conductivity and capacity of snow. Note the diffusivity is calculated based on the posterior distributions from Figures 2a and 2b; (d) heat conductivity of the boundary layer, (e) the insulation factor, (f) saturated soil water content, (g) the fraction of water losses, (h) surface albedo in nonsnow covered season, (i) the factor reflects vegetation impacts on snow melting, (j) factor affects snow sublimation rate, (k) snow density, and (l) aging factor on snow melting.

temperature according to each of the treatment starting from June 2014 and adding air temperature starting from August 2015 in model simulations. In model simulations, soil temperatures were read from the control simulation plus the corresponding warming treatments (e.g., +2.25°C, +4.5°C, +6.75°C, and +9°C) instead of explicitly tracking the manipulative heat additions. Other climate variables for warming treatment simulations (June 2014 to August 2016) are available in *Hanson et al*. [2015] and *Hanson et al*. [2016b] in addition to sources mentioned in previous sections.

It is difficult to separate the sensitivity of soil temperature to air warming from the field manipulation protocol as heat is constantly added in the whole ecosystem warming treatment to sustain targeted soil temperatures. In addition to mimic the SPRUCE field warming protocols, we tested the sensitivity of soil temperature to air warming through increasing air temperature by 0°C (control), 2.25°C, 4.5°C, 6.75°C, and 9°C, respectively. This sensitivity test provides information on how soil temperature responses to air temperature considering snow dynamics and freeze-thaw cycles. In this test, we ran the model forward for 4 years (after the 2011–2014 data assimilation period) for diagnostic purpose. The monthly average response, that is, the difference between each warming treatment and the control, was used to indicate the sensitivity.

3. Results

3.1. Posterior Distribution of Parameters

The snow density (ρ_{snow}) and the aging factor that affects snow melting (m) (Figure 2) are well constrained with bell shape posterior distributions. The heat capacity of snow (C_{snow}, Figure 2a), heat conductivity of

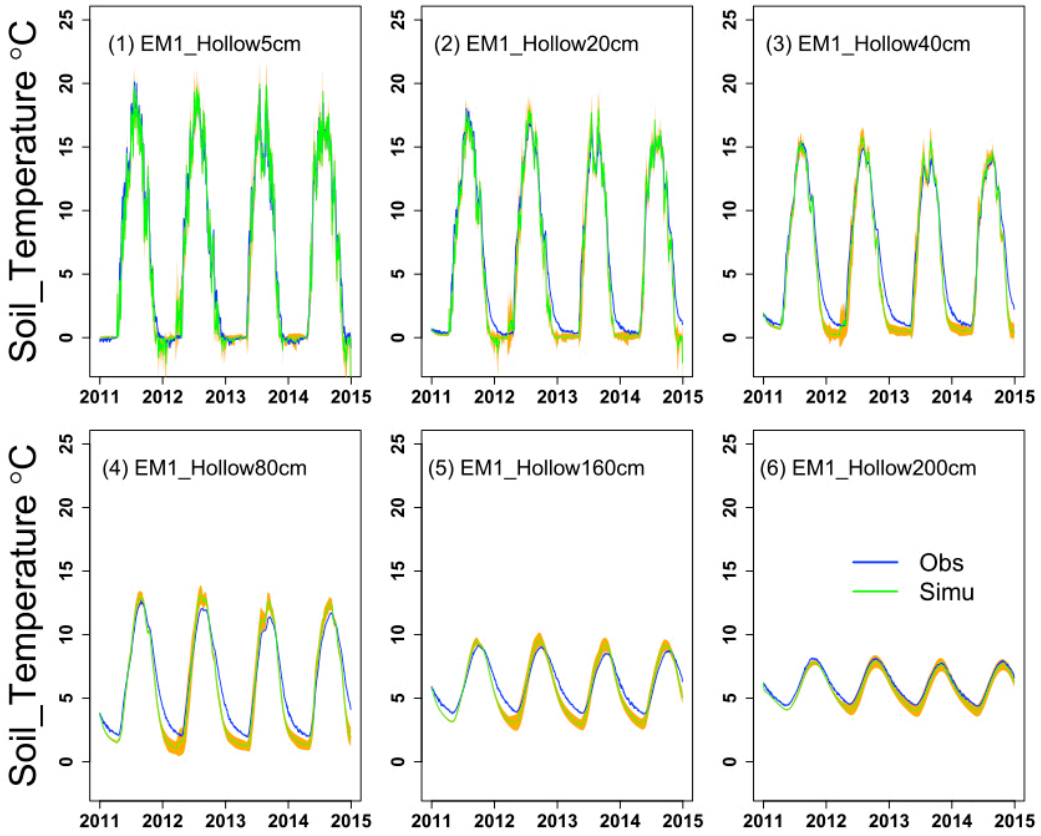

Figure 3. Simulated mean (green lines) versus observed soil temperature (blue lines) for different soil layers over 2011–2014. The shading orange area corresponds to the 1 standard deviation based on 100 randomly chosen model simulations with parameters drawn from the posterior distributions.

snow (k_{snow}, Figure 2b), the boundary heat conductivity ($k_{boundary}$, Figure 2c), the vegetation factor on snow melting (fv, Figure 2i), and the empirical factor on snow sublimation (f_{sub}, Figure 2j) are edge hitting, limited by their physical constraints. Although the heat conductivity and capacity of snow are edge hitting, their ratio (i.e., the diffusivity, Figure 2c) is relatively well constrained. The shape of the saturated soil water content (θ_{sat}, Figure 2f), the fraction of standing water lost as runoff or lateral flows ($r_{percent}$, Figure 2g), and the surface albedo (α, Figure 2h) are relatively flat as we do not have direct data to constrain these parameters.

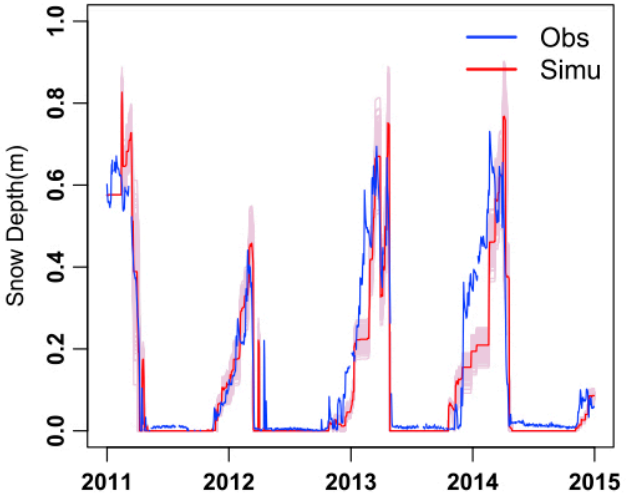

Figure 4. Simulated mean (red line) versus observed snow depth (blue line) from 2011 to 2014. Pink lines correspond to 100 randomly chosen model simulations with parameters drawn from the posterior distributions.

3.2. Simulated Soil Temperature, Snow Depth, and Frozen Depth

Simulated soil temperature captures the diurnal and seasonal patterns from observed soil temperature from different soil layers (Figure 3). In line with observations, variation in soil temperature is stronger in shallow soil layers

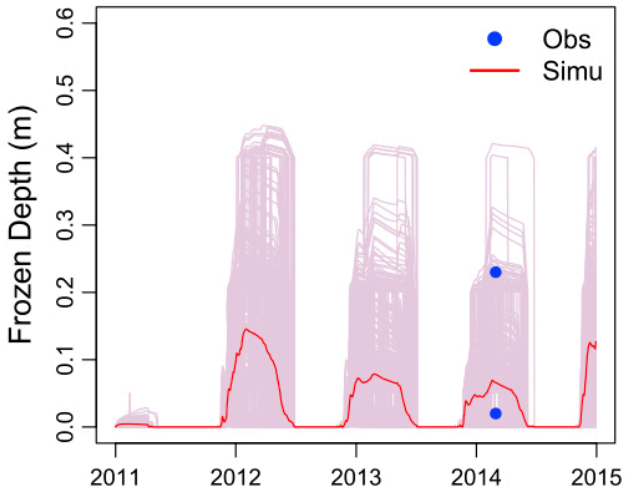

Figure 5. Simulated mean (red line) versus observed frozen depth (blue dots) from 2011 to 2014. Pink lines correspond to 100 randomly chosen model simulations with parameters drawn from the posterior distributions. Observations show the range of frozen depth along a transect measured in February 2014.

compared to deep soil layers. Performance of TECO is better at 5 cm and 200 cm depths compared to other soil depths. When we plot the simulated soil temperature against observed soil temperature, points spread evenly around the 1:1 line, with a regression slope of 1.06 ($R^2 = 0.97$). The uncertainty (represented by 1 standard deviation) from simulation is generally small.

The timing of simulated snowfall and snowmelt is generally consistent with the observation (Figure 4). Maximum snow depths in different years are reasonable from the snow module compared to observation. However, there are some mismatches between model simulation and observation. For example, the model fails to capture the sudden increase in snow depth during the winter of 2013 since there is no sudden increase in precipitation (therefore, snowfall) in observed forcing for snow accumulation (Figure 4).

Observed frozen depth was measured along a transect (10 points) in the bog in February, 2014, which ranged from 3 cm to 23 cm. Our 100 realizations of model simulation (correspond to 100 randomly selected parameter sets) display a large range in simulated frozen depth for years 2012–2014 (Figure 5). In February 2014, the simulated range of frozen depth is larger than the reported range based on observation from one transect. The mean frozen depth for each year is comparable with observation, with the highest frozen depth in year 2012 and lowest in year 2011 (Figure 6). The observed frozen depths are smaller than the means from model simulations in years 2012, 2013, but within ±1 standard deviations of model simulations. Model slightly overestimates the frozen depth in year 2011.

3.3. Validation and Forecast

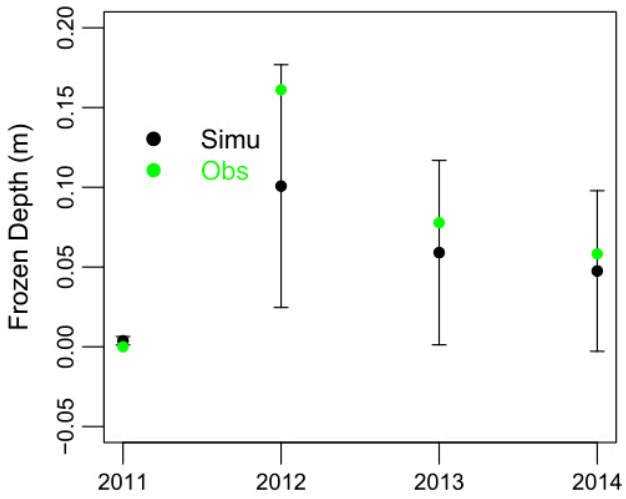

Figure 6. Modeled (black dots) versus observed annual mean (green dots) frozen depth in different years. Error bars correspond to 1 standard deviations from 100 randomly chosen model simulations with parameters drawn from the posterior distributions.

Observation from January 2015 to August 2016 serves to validate model forecasting, which is independent from the data assimilation stage in which observed soil temperature from 2011 to 2014 (pretreatment) is used to constrain model parameters. During the period of January 2015 to August 2016, forecasted soil temperature matches observed soil temperature following a similar pattern as in the data assimilation stage (Figures 3 and 7). TECO slightly overpredicts the 5 cm soil temperature in the summer of 2015; however, the uncertainty in forecasted soil temperature is relatively large in summer (compared to spring and autumn) and observation generally falls within the range forecasted by TECO. While the forecasting uncertainty is

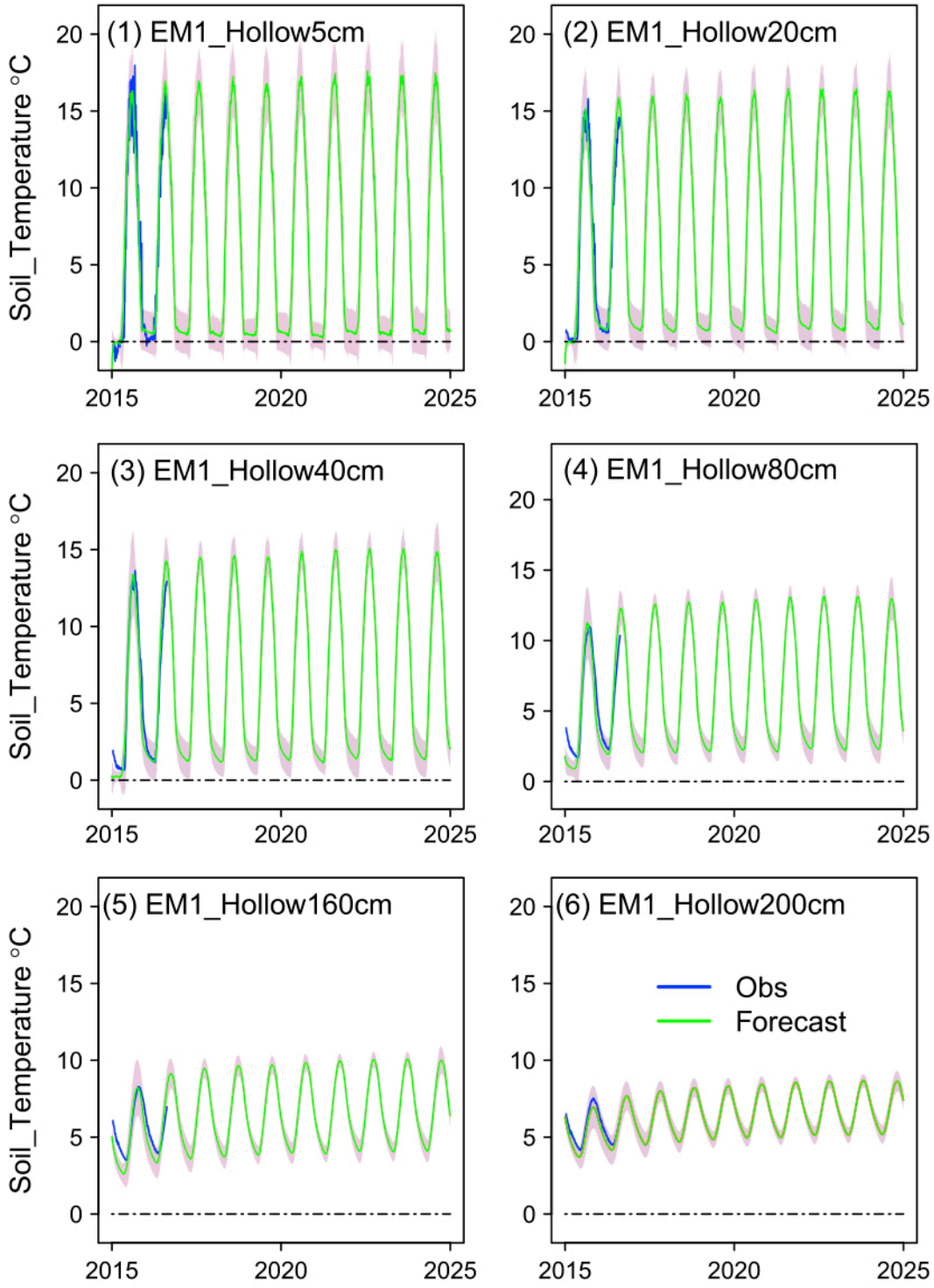

Figure 7. Forecasting of soil temperature dynamics for different soil layers based on stochastically generated weather forcing. Green lines indicate mean model forecasting from 2015–2024. And blue lines represent observations from 2015 to current (August 2016) during the validation period. Shading pink area correspond to forecasting uncertainty (1 standard deviation) due to randomly chosen forcing and parameters.

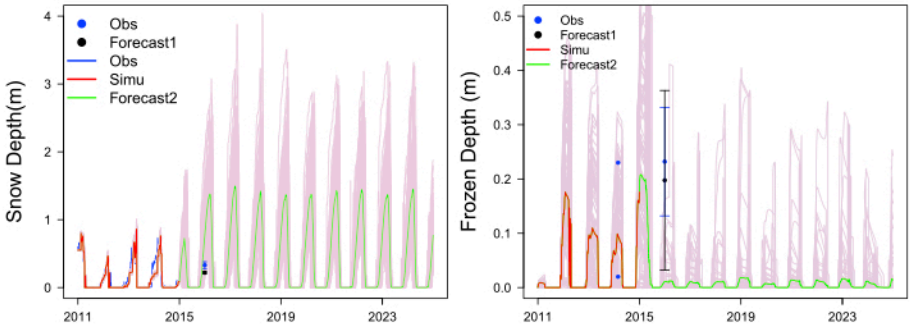

Figure 8. Forecasting of (left) snow depth and (right) frozen depth. Green lines indicate means from model forecasting (2015–2024) with stochastically generated weather. Red lines correspond to mean model simulations for SPRUCE pre-treatment stage (2011–2014) in which observations (soil temperature and snow depth) are used to constrain model parameters through data assimilation. Pink lines correspond to 100 realizations with randomly chosen forcing and parameters. Pink lines indicate possible simulated range generated by models. And blue lines or dots represent observations. Black dots are forecasting with measured weather forcing. Error bars correspond to 1 standard deviations.

relatively large in summer and winter in the 5 cm soil layer compared to spring and autumn, the forecasting uncertainty spreads more evenly among different seasons at the 2 m soil depth in 2015. There is a slight increasing trend in forecasted soil temperature over the 10 year forecasting period for each soil layer.

Simulated snow depth for January 2016 (black dot, 0.33 ± 0.05 m) is comparable with observation if forcing is prescribed the same as observation (Figure 8). And the uncertainty caused by parameters is small. Forecasting that takes into account both parameter and forcing uncertainty overestimates snow depth by 0.44 m (green lines). The overall uncertainty in forecasted snow depth is relatively large, with a maximum snow depth approaching 4 m during the 2015–2024 period.

Similarly, the forecasted frozen depth with prescribed forcing is comparable with observation obtained for January 2016 although the uncertainty from forecasting with different parameter sets is high (Figure 8). The observed frozen depth is 0.23 ± 0.10 m while the forecasted frozen depth is 0.20 ± 0.17 m. Forecasting that takes into account both parameter and forcing uncertainty greatly underestimates frozen

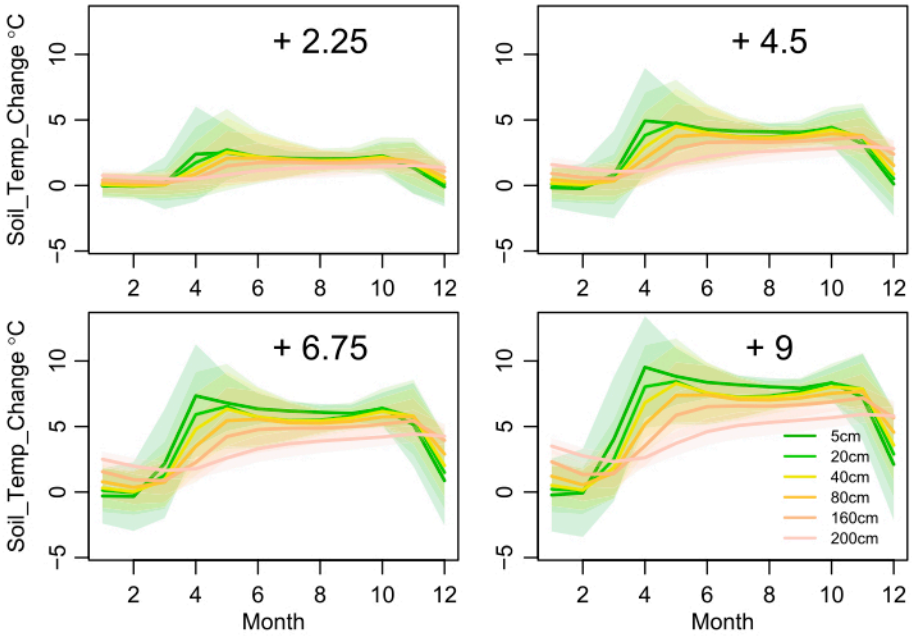

Figure 9. Response of soil temperature to air temperature warming. Different panels correspond to different warming treatments. Colored lines indicate different soil depths. Shading areas correspond to response uncertainty based on 100 simulations with randomly chosen parameters from their posterior distributions.

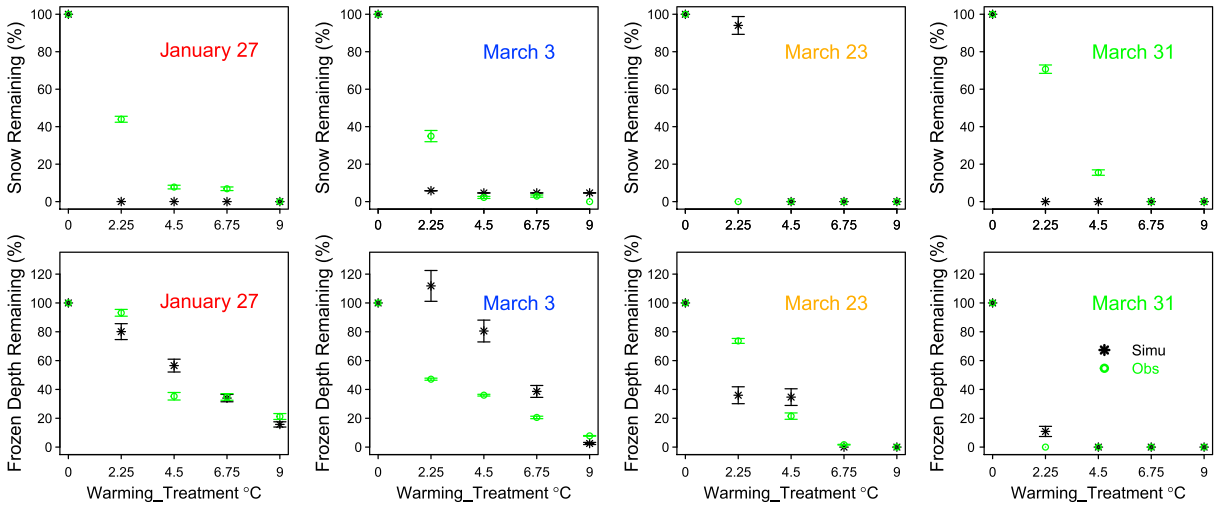

Figure 10. Responses of (top row) snow and (bottom row) frozen depths to whole ecosystem warming treatments (peat + air warmings) in 4 days in 2016 when observations are available. The *x* axis is the warming treatment (°C) and *y* axis represent the relative snow (Figure 10, top row) or frozen depth (Figure 10, bottom row) in percentage compared to the control (0°C treatment). Black stars are results from model simulations and green dots are from observations. Error bars correspond to 1 standard deviations from 100 random draws using nonparametric bootstrapping.

depth. And the predicted frozen depth is generally small (<0.1 m) after 2015 if forecasting is conducted with stochastically generated weather forcing.

3.4. Response to Warming

As shown in Figure 9, the response of soil temperature to air warming varies with time and soil depth. Soil temperature generally responds more strongly to summer warming compared to winter warming largely due to the presence of snow and ice in winter. Among different soil layers, deep soil layers show stronger temperature response in winter, while shallow soil layers are more sensitive to summer warming compared to winter. The direction of winter warming impact remains largely uncertain with both increase and reduction in soil temperature especially for surface soil layers, depending on the snow cover. Among different warming treatments, higher air temperature generally results in higher average soil temperature.

In line with SPRUCE whole ecosystem warming manipulations (peat + air warmings), snow depth is reduced with different warming treatments (Figure 10). TECO reproduces the observed relative (compared to +0.0°C) small snow depths in 2016 when warming treatment is no smaller than +4.5°C. However, TECO underestimates the relative snow depths on 27 January, 3 March, and 31 March 31 while overestimated the relative snow depth on 23 March. There is no snow remains in the +9°C treatment from observations, which is generally reproduced from TECO except on 3 March with 5% snow remaining.

TECO generally captures the relative frozen depths in response to different whole ecosystem warming treatments (peat + air warmings) in different days of 2016 when observations are available (Figure 10). However, TECO overestimates the relative soil frozen depths in the +2.25°C treatment on 3 March and 31 March, while underestimates the relative frozen depths on 27 January and 31 March 31. Overestimations of frozen depth are also evident for the +4.5°C treatment on 27 January and 3 March and 23 March.

4. Discussion

We combined detailed measurements and process-based simulation of soil temperature through data assimilation before forecasting soil temperature dynamics in the coming ~10 years at the SPRUCE plot. As a first step, we also explored the plausible response directions of soil thermal dynamics through mimicking field warming treatments. The soil temperature module in TECO captures overall patterns of soil temperature, snow, and freeze-thaw dynamics in data assimilation and validation/forecasting stages. Here we discuss simulated soil temperature dynamics and implications for better understanding and forecasting of soil biogeochemical dynamics.

4.1. Model Performance

For simulated soil temperature, the performance is good especially at surface (5 cm) and bottom (200 cm) layers. The top 5 cm soil temperature depends more on air temperature and the top boundary layer conditions (compared to deeper soil layers), which are constrained through data. The 200 cm soil temperature relies more on the model structure, such as the bottom layer location. *Zhang et al*. [2008] revealed that the depth of soil column affected soil temperature simulation in a boreal aspen forest. *Alexeev et al*. [2007] discussed the importance of soil layer configuration and column depth on simulating soil temperature in permafrost region using CLM3. We also tested different bottom boundary layer locations (data not shown) assuming very small (almost 0) heat exchange at the bottom boundary layer. The impact of boundary layer location on near term (e.g., 5 years) soil temperature forecasting is small since forecasting through data assimilation relies partly on information from observations. However, as in *Alexeev et al*. [2007], soil column thickness affects long-term (e.g., 100 years) soil temperature predictions. Thinner soil shows a stronger warming trend when TECO is forced with long term weather forcing (e.g., 100 years) since less soil is available to store and buffer heat changes from CMIP5. The slight warming trend in 10 year forecasting with stochastically generated weather forcing may partly reflect the slow change of soil thermal dynamics to evolving ecosystem conditions as vegetation status and soil carbon are not in steady state.

Soil temperatures of middle layers come out from interactions among heat transfer, freeze-thaw cycle, and soil water dynamics especially when the heat conductance and capacity in each soil layer are dynamically linked with different soil components in TECO. Mismatches (compared to observations) in middle layer soil temperature simulations are likely to be reduced if free variables are brought to dynamically adjust middle layer heat conductance and capacity according to observations. Although no parameter is adjusted through data assimilation for middle layers in the current setup, TECO is sufficient in capturing middle layer soil temperatures.

Snow depth and frozen depth can be reasonably reproduced by TECO with appropriate weather forcing. Deep snow depth generally indicates shallower frozen depth due to the insulation effect of snow [*Zhang*, 2005; *Yi et al*., 2015]. Similar to observations, TECO simulates almost no frost in the year 2011 (with deep snow) and strong frozen depth in 2012 (with shallow snow). Although the prediction accuracy for snow depth and frozen depth is lower compared to that for soil temperature with stochastically generated weather forcing, results are comparable with measurements when forecasting is conducted with observed weather variables during 2015–2016. Snow depth and frozen depth are more sensitive to the accuracy of forecasted weather conditions. The stochastic weather generator creates synthetic weather data based on characteristics of historical observed weather conditions. The accuracy of the generated weather forcing is difficult to assess. Figure S1 compares the stochastically generated air temperature and precipitation with these from the Earth system models that participated in CMIP5 on a daily time scale. Air temperature is generally in line, while precipitation varies largely between these two approaches. The forecasted mean snow depth and frozen depth are closer to observations but with even larger uncertainties if we conducted forecasting with forcing from CMIP5 (data not shown), partly due to the large variations in forecasted weather among these models. Nevertheless, TECO is adequate for short-term (such as weekly) snow depth and frozen depth forecasting if we take advantage of the reliability of near-real-time weather forecasting.

Snow depth and frozen depth from TECO generally respond to air warming and deep peat warming in a similar direction as from observations. As expected, air warming and deep soil warming together reduce snow depth and frozen depth. The quick reduction of snow depth in +2.25°C treatment on 27 January does not strongly reduce the frozen depth with both positive effect from higher-energy input and negative effect of reduced snow insulation. Although it is intuitive that future climate warming is likely to cause warmer soils, *Groffman et al*. [2001] proposed colder soils in a warmer world in snow seasons since warming reduces snow cover based on their experimental results. Removal of the snow cover is reported to decrease soil temperature with reduced snow insulation effect from different studies [*Pilon et al*., 1994; *Groffman et al*., 2001]. As a result, the interaction between frozen depth, snow depth, and warming is nonlinear. We represented both deep peat heating and air warming in TECO simulations but did not track the heating processes conducted in SPRUCE explicitly. For example, we did not take into account the time required to reach the treatment level after initialization of the warming experiment, which may contribute to mismatches between modeled and observed responses. In addition, we assume that observed field level responses come only from the

treatment effect while in fact field responses are afflicted by the background differences such as the species composition and the microtopography.

4.2. Model Structure and Parameterization

Parameters such as the heat conductivity and capacity are known to directly regulate soil thermal dynamics through the heat diffusivity (i.e., the ratio between conductivity and capacity). The heat diffusivity of snow is well constrained through data assimilation in this study. We did not parameterize the heat capacity and conductivity in different soil layers to better match middle soil layer soil temperature observations. Instead, the current model setup adopts the approach that relies largely on the physical properties of the soil systems with minimal parameters to be tuned. Soil thermal properties of each individual components are relatively well known, especially for air, ice, and water. The mineral component of the peat is slight [*Verry et al*., 2011], and the thermal properties of the solid phase (nonice) of soil largely reflect these from organic matter, which varies in a small range [*Farouki*, 1981; *Lawrence and Slater*, 2008]. We use the volume to weight the contribution of each soil component to the overall heat conductivity and capacity in each soil layer. Such approach is simple but may not capture the integrated soil thermal properties best. For example, some researches applied the geometric mean to weight different components [*Farouki*, 1981; *Lawrence and Slater*, 2008].

Snow and ice are important in regulating thermal dynamics of this northern peatland. With detailed snow depth observations, snow density that plays a key role in transferring snow water equivalent into snow depth is well constrained by data. We did not explicitly track physical processes that may alter snow density due to lack of sufficient data. Snow density may change as snow ages, such as through metamorphism [*Pomeroy and Brun*, 2001]. Nevertheless, our current approach is sufficient based on available data. We only have several data points in ice-related observations, and these data points are associated with large uncertainty. In addition, the ice content or frozen depth is emergent from soil thermal dynamics. Ice forms as soil temperature drops below zero, and the amount of ice that can be formed depends on soil available water content, soil temperature, and the thermal budgets. Parameters that directly regulate ice formation, such as the latent heat of fusion, are generally physical constants. We therefore did not incorporate ice related observations into our data assimilation. Instead, ice related observations are used to diagnose the model performance.

The soil thermal module presented in this study is only one part of the complex ecosystem model that couples hydrology, biogeochemical cycles, and energy dynamics. Factors or processes that alter different aspects of the model have indirect impacts on soil thermal dynamics. For example, nitrogen availability regulates plant photosynthesis, which modifies evapotranspiration loss of soil water and the surface energy budgets. Soil hydrology is linked to middle layer soil thermal conductivity and capacity as well as soil thermal dynamics in ice-water transitions. However, parameters related to surface energy budgets (nonsnow covered albedo, α) and the hydrological properties (the saturated soil water content θ_{sat} and the fraction of water losses $r_{percent}$) are not well constrained through data assimilation. The regulation of surface albedo in nonsnow covered season is likely to be compensated by the boundary heat conductivity when assimilating observed soil temperature. Previous studies from *Shi et al*. [2015] revealed that the water table seldom drops below 30 cm during 2011–2014. The range of $r_{percent}$ is chosen to reflect the relatively high moisture content in this peatland. Under current conditions, changes in soil water content and the impact on soil thermal dynamics are not dramatic. However, future warming is likely to significantly alter peatland soil hydrology and its impact on soil thermal dynamics. More soil hydrological or surface energy related observations are needed to thoroughly constrain and quantify their impacts on soil thermal dynamics.

4.3. Nonuniform Response of Soil Temperature to Air Warming

We showed in this study that air warming triggered differentiated responses of soil temperature. These differentiated responses may obscure the temperature sensitivity of SOM decomposition [*Rustad et al*., 2001; *Davidson and Janssens*, 2006]. Despite that the scientific community has spent considerable efforts in understanding how soil organic carbon responds to warming, the magnitude and direction of warming induced soil carbon changes remain controversial [*Arora et al*., 2013; *Liang et al*., 2015]. Many factors, such as SOM composition [*Xu et al*., 2012], soil microbial activities [*Allison et al*., 2010], and methodology concerns [*Liang et al*., 2015], are reported to contribute to the temperature sensitivity of SOM decomposition. Since air warming can induce different warming effects in soil temperature in different soil layers or during different time in a year, manipulative experiments based on air warming, such as through field chambers, may incorporate

responses from soil temperature itself in addition to the temperature sensitivity of SOM if soil temperature is extrapolated from air warming.

Our result also posted a question on using a single-layer soil temperature to represent the whole soil temperature dynamics especially when deep soil is involved such as in studies carried out in peatland and permafrost regions. With strong radiative forcing, heat generally transfers from the upper soil layer to the lower soil layer in summer. Heat that is available for rising soil temperature is reduced as it transfers along the soil profile since some heat is used to increase the upper soil layer temperature. As a result, the response to air warming is stronger from the upper soil layer compared to the lower soil layer. Deep soil layer temperature is more uniform between seasons and the winter soil temperature in deep layers may carry lagged impact from warmer seasons. Winter soil temperature dynamics are actually more complex when snow and frozen soil are involved. Warming treatment reduces snow depth and therefore the insulation effect of snow. Certain amount of air warming may actually reduce soil temperature especially in the uppermost soil layer as shown by the negative value in this study. If the top soil layer response is applied to deep soil layers, warming response is likely to be overestimated in summer.

4.4. Limitations and Moving Forward

Although the SPRUCE field plots are well selected to minimize background differences caused by heterogeneities in vegetation and soil and to focus on response patterns and mechanisms in a regression-based design, detailed studies on thermal dynamics require plot-specific data to constrain the model. In addition to background heterogeneities, different warming treatments are likely to result in divergent alternations in vegetation growth, energy transfer and hydrological cycles, and therefore different mechanisms in regulating soil thermal dynamics. For example, the snow cover is almost zero in the +9.0°C treatment year round and soil thermal responses might be different from plots with snow cover. As observations accumulate, detailed studies that apply our current data assimilation approach will provide more information on how soil thermal dynamics response and feedback to ecosystem dynamics at the SPRUCE site. However, the reliance on detailed field monitoring limits its application to other sites or to a large scale since belowground soil states is heterogeneous and not widely measured.

One of the motivations to improve soil thermal studies is to facilitate the predictions of terrestrial biogeochemical cycles. SOM is an important but largely uncertain component in terrestrial carbon cycle [*Friedlingstein et al*., 2006], and improvements in model structure, parameterization, and external forcing are key steps toward realistic projection of SOM dynamics [*Luo et al*., 2016]. Here we focus on soil temperature. We argue for the importance of monitoring and simulating soil temperature dynamics in order to better understand SOM dynamics since the response of soil temperature itself to global changes is nonuniform. As the current soil thermal module is configured within the ecosystem model framework, future studies can quantify the extent that biogeochemical studies benefit from improved soil thermal understandings. The web-based EcoPAD we developed for the SPRUCE project (http://ecolab.cybercommons.org/ecopad_portal/) can provide some improvement. As the 10 year long SPRUCE research project goes on, EcoPAD can constantly fetch new observations and assimilate these observations into TECO to update model parameters and forecast future dynamics in a most informed manner similarly to the weather forecasting. With future EcoPAD forecasting of both soil thermal and biogeochemical states, it is feasible to provide a detailed picture about the impacts of soil thermal conditions on SOM dynamics.

5. Conclusions

We developed a soil temperature module inside Terrestrial ECOsystem (TECO) model that takes into account snow dynamics, underground heat transfer among different soil layers, and during freeze and thaw events. After detailed observations were combined with TECO by data assimilation techniques, we forecasted soil temperature dynamics in the Spruce and Peatland Responses Under Climatic and Environmental change (SPRUCE) experimental site. Our results demonstrated that with appropriate weather forcing, soil temperature can be reasonably forecasted and is beneficial to carbon forecasting studies. Uncertainty is smaller for forecasting soil temperature but large for snow and frozen depths. In addition, we call for caution when extrapolating manipulative air warming experiments to understand warming impact on soil organic matter decomposition since soil temperature responds nonuniformly to air warming with higher elevated soil temperature in summer than winter and stronger warming in shallow than deep soil layers in summer.

Acknowledgments
This work is primarily supported by subcontract 4000144122 from Oak Ridge National Laboratory (ORNL) to the University of Oklahoma. ORNL's work is supported by the U.S. Department of Energy (DOE), Office of Science, Office of Biological, and Environmental Research. Oak Ridge National Laboratory is managed by UT-Battelle, LLC, for the U.S. Department of Energy under contract DE-AC05-00OR22725. Research in Yiqi Luo's EcoLab was also financially supported by U.S. DOE DE-SC0008270 and DE-SC00114085 and U.S. National Science Foundation (NSF) grant EF 1137293 and OIA-1301789. Relevant measurements were obtained from the SPRUCE webpage (http://mnspruce.ornl.gov/) or the archived ftp site (ftp://sprucedata.ornl.gov). Source code of the TECO thermal model is available at http://ecolab.ou.edu/download/Huang2017JGR.php. Additional data sets are available in the supporting information.

References

Alexeev, V. A., D. J. Nicolsky, V. E. Romanovsky, and D. M. Lawrence (2007), An evaluation of deep soil configurations in the CLM3 for improved representation of permafrost, *Geophys. Res. Lett.*, *34*, L09502, doi:10.1029/2007GL029536.

Allison, S. D., M. D. Wallenstein, and M. A. Bradford (2010), Soil-carbon response to warming dependent on microbial physiology, *Nat. Geosci.*, *3*(5), 336–340, doi:10.1038/ngeo846.

Arora, V. K., et al. (2013), Carbon-concentration and carbon-climate feedbacks in CMIP5 earth system models, *J. Clim.*, *26*(15), 5289–5314, doi:10.1175/jcli-d-12-00494.1.

Ball, J. T., I. E. Woodrow, and J. A. Berry (1987), A model predicting stomatal conductance and its contribution to the control of photosynthesis under different environmental conditions, in *Progress in Photosynthesis Research*, edited by J. Biggens, pp. 221–224, Martinus Nijhoff, Zoetermeer, Netherlands.

Betts, A. K., and J. H. Ball (1997), Albedo over the boreal forest, *J. Geophys. Res.*, *102*, 28,901–28,909, doi:10.1029/96JD03876.

Ciais, P., et al. (2013), Carbon and other biogeochemical cycles, in *Climate Change 2013: The Physical Science Basis. Contribution of Working Group I to the Fifth Assessment Report of the Intergovernmental Panel on Climate Change*, edited by T. F. Stocker et al., pp. 465–570, Cambridge Univ. Press, Cambridge, U. K., and New York.

Davidson, E. A., and I. A. Janssens (2006), Temperature sensitivity of soil carbon decomposition and feedbacks to climate change, *Nature*, *440*(7081), 165–173, doi:10.1038/nature04514.

DeGaetano, A. T., D. S. Wilks, and M. McKay (1996), A physically based model of soil freezing in humid climates using air temperature and snow cover data, *J. Appl. Meteorol.*, *35*(6), 1009–1027, doi:10.1175/1520-0450(1996)035<1009:apbmos>2.0.co;2.

Elberling, B., C. Nordstrom, L. Grondahl, H. Sogaard, T. Friborg, T. R. Christensen, L. Strom, F. Marchand, and I. Nijs (2008), High-arctic soil CO_2 and CH_4 production controlled by temperature, water, freezing and snow, in *Advances in Ecological Research, Vol 40: High-Arctic Ecosystem Dynamics in a Changing Climate*, edited by H. Meltofte et al., pp. 441–472, Elsevier, Amsterdam.

Euskirchen, E. S., et al. (2006), Importance of recent shifts in soil thermal dynamics on growing season length, productivity, and carbon sequestration in terrestrial high-latitude ecosystems, *Global Change Biol.*, *12*(4), 731–750, doi:10.1111/j.1365-2486.2006.01113.x.

Farouki, O. T. (1981), *Thermal properties of soil, Cold Regions, Monograph*, pp. 81-1, Research & Engineering Lab., Hanover.

Farquhar, G. D., S. V. Caemmerer, and J. A. Berry (1980), A biochemical-model of photosynthetic CO_2 assimilation in leaves of C_3 species, *Planta*, *149*(1), 78–90, doi:10.1007/bf00386231.

Friedlingstein, P., et al. (2006), Climate-carbon cycle feedback analysis: Results from the C^4MIP model intercomparison, *J. Clim.*, *19*(14), 3337–3353, doi:10.1175/jcli3800.1.

Ge, Y., and G. Gong (2010), Land surface insulation response to snow depth variability, *J. Geophys. Res.*, *115*, D08107, doi:10.1029/2009JD012798.

Gelman, A., and D. B. Rubin (1992), Inference from iterative simulation using multiple sequences, *Stat. Sci.*, *7*, 457–511.

Gelman, A., J. B. Carlin, H. S. Stern, and D. B. Rubin (2003), *Bayesian Data Analysis*, 2nd ed., Chapman&Hall/CRC, Boca Raton, Fla.

Granberg, G., H. Grip, M. O. Lofvenius, I. Sundh, B. H. Svensson, and M. Nilsson (1999), A simple model for simulation of water content, soil frost, and soil temperatures in boreal mixed mires, *Water Resour. Res.*, *35*, 3771–3782, doi:10.1029/1999WR900216.

Groffman, P. M., C. T. Driscoll, T. J. Fahey, J. P. Hardy, R. D. Fitzhugh, and G. L. Tierney (2001), Colder soils in a warmer world: A snow manipulation study in a northern hardwood forest ecosystem, *Biogeochemistry*, *56*(2), 135–150, doi:10.1023/a:1013039830323.

Hanson, P. J., J. S. Riggs, C. Dorrance, and L. A. Hook (2011), *SPRUCE Environmental Monitoring Data: 2010–2011*, O. R. N. L. Carbon Dioxide Information Anal. Center, U.S. Department of Energy, Oak Ridge, Tenn.

Hanson, P. J., J. S. Riggs, W. R. Nettles, M. B. Krassovski, and L. A. Hook (2015), *SPRUCE Deep Peat Heating (DPH) Environmental Data, February 2014 through July 2015*, Carbon Dioxide Information Analysis Center, Oak Ridge Natl. Lab., U.S. Department of Energy, Oak Ridge, Tenn.

Hanson, P. J., A. L. Gill, X. Xu, J. R. Phillips, D. J. Weston, R. K. Kolka, J. S. Riggs, and L. A. Hook (2016a), Intermediate-scale community-level flux of CO2 and CH4 in a Minnesota peatland: Putting the SPRUCE project in a global context, *Biogeochemistry*, *129*(3), 255–272, doi:10.1007/s10533-016-0230-8.

Hanson, P. J., J. S. Riggs, W. R. Nettles, M. B. Krassovski, and L. A. Hook (2016b), *SPRUCE Whole Ecosystems Warming (WEW) Environmental Data Beginning August 2015*, O. R. N. L. Carbon Dioxide Information Analysis Center, U.S. Department of Energy, Oak Ridge, Tenn.

Hanson, P. J., J. S. Riggs, W. R. Nettles, J. R. Phillips, M. B. Krassovski, L. A. Hook, A. D. Richardson, D. M. Ricciuto, J. M. Warren, and C. Barbier (2016c), Achieving whole-ecosystem warming using air and deep soil heating methods with an elevated CO_2 atmosphere, *Biogeosci. Discuss.*, doi:10.5194/bg-2016-449.

Hopmans, J. W., and J. H. Dane (1986), Temperature-dependence of soil hydraulic-properties, *Soil Sci. Soc. Am. J.*, *50*(1), 4–9.

Jungqvist, G., S. K. Oni, C. Teutschbein, and M. N. Futter (2014), Effect of climate change on soil temperature in Swedish boreal forests, *PLoS One*, *9*(4), doi:10.1371/journal.pone.0093957.

Kalnay, E. (2002), *Atmospheric Modeling, Data Assimilation and Predictability*, Cambridge Univ. Press, Cambridge, U. K., and New York.

Kolka, R. K., S. D. Sebestyen, E. S. Verry, and K. N. Brooks (2011), *Peatland Biogeochemistry and Watershed Hydrology at the Marcell Experimental Forest*, p. 488, CRC Press, Boca Raton, Fla.

Koven, C. D., B. Ringeval, P. Friedlingstein, P. Ciais, P. Cadule, D. Khvorostyanov, G. Krinner, and C. Tarnocai (2011), Permafrost carbon-climate feedbacks accelerate global warming, *Proc. Natl. Acad. Sci. U.S.A.*, *108*(36), 14,769–14,774, doi:10.1073/pnas.1103910108.

Koven, C. D., W. J. Riley, and A. Stern (2013), Analysis of permafrost thermal dynamics and response to climate change in the CMIP5 Earth system models, *J. Clim.*, *26*(6), 1877–1900, doi:10.1175/jcli-d-12-00228.1.

Krassovski, M. B., J. S. Riggs, L. A. Hook, W. R. Nettles, P. J. Hanson, and T. A. Boden (2015), A comprehensive data acquisition and management system for an ecosystem-scale peatland warming and elevated CO_2 experiment, *Geosci. Instrum. Methods Data Syst.*, *4*(2), 203–213, doi:10.5194/gi-4-203-2015.

Lawrence, D. M., and A. G. Slater (2008), Incorporating organic soil into a global climate model, *Clim. Dyn.*, *30*(2–3), 145–160, doi:10.1007/s00382-007-0278-1.

Li, C. S., J. Aber, F. Stange, K. Butterbach-Bahl, and H. Papen (2000), A process-oriented model of N_2O and NO emissions from forest soils: 1. Model development, *J. Geophys. Res.*, *105*, 4369–4384, doi:10.1029/1999JD900949.

Liang, J. Y., D. J. Li, Z. Shi, J. M. Tiedje, J. Z. Zhou, E. A. G. Schuur, K. T. Konstantinidis, and Y. Q. Luo (2015), Methods for estimating temperature sensitivity of soil organic matter based on incubation data: A comparative evaluation, *Soil Biol. Biochem.*, *80*, 127–135, doi:10.1016/j.soilbio.2014.10.005.

Luo, L. F., et al. (2003), Effects of frozen soil on soil temperature, spring infiltration, and runoff: Results from the PILPS 2(d) experiment at Valdai, Russia, *J. Hydrometeorol.*, *4*(2), 334–351, doi:10.1175/1525-7541(2003)4<334:eofsos>2.0.co;2.

Luo, Y., R. S. Loomis, and T. C. Hsiao (1992), Simulation of soil-temperature in crops, *Agric. For. Meteorol.*, *61*(1–2), 23–38, doi:10.1016/0168-1923(92)90023-w.

Luo, Y., K. Ogle, C. Tucker, S. Fei, C. Gao, S. LaDeau, J. S. Clark, and D. S. Schimel (2011), Ecological forecasting and data assimilation in a data-rich era, *Ecol. Appl.*, *21*, 1429–1442.

Luo, Y. Q., et al. (2016), Toward more realistic projections of soil carbon dynamics by Earth system models, *Global Biogeochem. Cycles*, *30*, 40–56, doi:10.1002/2015GB005239.

Mackiewicz, M. C. (2012), A new approach to quantifying soil temperature responses to changing air temperature and snow cover, *Pol. Sci.*, *6*(3–4), 226–236, doi:10.1016/j.polar.2012.06.003.

Melillo, J. M., P. A. Steudler, J. D. Aber, K. Newkirk, H. Lux, F. P. Bowles, C. Catricala, A. Magill, T. Ahrens, and S. Morrisseau (2002), Soil warming and carbon-cycle feedbacks to the climate system, *Science*, *298*(5601), 2173–2176, doi:10.1126/science.1074153.

Park, H., A. B. Sherstiukov, A. N. Fedorov, I. V. Polyakov, and J. E. Walsh (2014), An observation-based assessment of the influences of air temperature and snow depth on soil temperature in Russia, *Environ. Res. Lett.*, *9*(6), doi:10.1088/1748-9326/9/6/064026.

Peng, S., et al. (2016), Simulated high-latitude soil thermal dynamics during the past 4 decades, *Cryosphere*, *10*(1), 179–192, doi:10.5194/tc-10-179-2016.

Pilon, C. E., B. Cote, and J. W. Fyles (1994), Effect of snow removal on leaf water potential, soil moisture, leaf and soil nutrient status and leaf peroxidase activity of sugar maple, *Plant Soil*, *162*(1), 81–88, doi:10.1007/bf01416092.

Pomeroy, J. W., and E. Brun (2001), Physical properties of snow, in *Snow Ecology: An Interdisciplinary Examination of Snow-Covered Ecosystems*, edited by H. G. Jones et al., pp. 46–126, Cambridge Univ. Press, Cambridge U. K., and New York.

Rawlins, M. A., R. B. Lammers, S. Frolking, B. M. Fekete, and C. J. Vorosmarty (2003), Simulating pan-Arctic runoff with a macro-scale terrestrial water balance model, *Hydrol. Processes*, *17*(13), 2521–2539, doi:10.1002/hyp.1271.

Roulet, N. T., P. M. Lafleur, P. J. H. Richard, T. R. Moore, E. R. Humphreys, and J. Bubier (2007), Contemporary carbon balance and late Holocene carbon accumulation in a northern peatland, *Global Change Biol.*, *13*(2), 397–411, doi:10.1111/j.1365-2486.2006.01292.x.

Rustad, L. E., J. L. Campbell, G. M. Marion, R. J. Norby, M. J. Mitchell, A. E. Hartley, J. H. C. Cornelissen, J. Gurevitch, and N. Gcte (2001), A meta-analysis of the response of soil respiration, net nitrogen mineralization, and aboveground plant growth to experimental ecosystem warming, *Oecologia*, *126*(4), 543–562.

Schaefer, K., T. J. Zhang, A. G. Slater, L. X. Lu, A. Etringer, and I. Baker (2009), Improving simulated soil temperatures and soil freeze/thaw at high-latitude regions in the simple biosphere/Carnegie-Ames-Stanford approach model, *J. Geophys. Res.*, *114*, F02021, doi:10.1029/2008JF001125.

Schuur, E. A. G., et al. (2015), Climate change and the permafrost carbon feedback, *Nature*, *520*(7546), 171–179, doi:10.1038/nature14338.

Sebestyen, S. D., C. Dorrance, D. M. Olson, E. S. Verry, R. K. Kolka, A. E. Elling, and R. Kyllander (2011), *Long-Term Monitoring Sites and Trends at the Marcell Experimental Forest*, CRC Press, Boca Raton, Fla.

Shi, X., P. E. Thornton, D. M. Ricciuto, P. J. Hanson, J. Mao, S. D. Sebestyen, N. A. Griffiths, and G. Bisht (2015), Representing northern peatland microtopography and hydrology within the community land model, *Biogeosciences*, *12*(21), 6463–6477, doi:10.5194/bg-12-6463-2015.

Shi, Z., Y. H. Yang, X. H. Zhou, E. S. Weng, A. C. Finzi, and Y. Q. Luo (2016), Inverse analysis of coupled carbon-nitrogen cycles against multiple datasets at ambient and elevated CO_2, *J. Plant Ecol.*, *9*(3), 285–295, doi:10.1093/jpe/rtv059.

Tfaily, M. M., W. T. Cooper, J. E. Kostka, P. R. Chanton, C. W. Schadt, P. J. Hanson, C. M. Iversen, and J. P. Chanton (2014), Organic matter transformation in the peat column at Marcell experimental Forest: Humification and vertical stratification, *J. Geophys. Res. Biogeosci.*, *119*, 661–675, doi:10.1002/2013JG002492.

Todd-Brown, K. E. O., J. T. Randerson, W. M. Post, F. M. Hoffman, C. Tarnocai, E. A. G. Schuur, and S. D. Allison (2013), Causes of variation in soil carbon simulations from CMIP5 earth system models and comparison with observations, *Biogeosciences*, *10*(3), 1717–1736, doi:10.5194/bg-10-1717-2013.

Todd-Brown, K. E. O., et al. (2014), Changes in soil organic carbon storage predicted by earth system models during the 21st century, *Biogeosciences*, *11*(8), 2341–2356, doi:10.5194/bg-11-2341-2014.

Toy, T. J., A. J. Kuhaida Jr., and B. E. Munson (1978), The prediction of mean monthly soil temperature from mean monthly air temperature, *Soil Sci.*, *126*, 96–104.

Verry, E. S., D. H. Boelter, J. Päivänen, D. S. Nichols, T. J. Malterer, and A. Gafni (2011), Physical properties of organic soils, in *Peatland Biogeochemistry and Watershed Hydrology at the Marcell Experimental Forest*, edited by R. K. Kolka et al., pp. 135–176, CRC Press, New York.

Wang, Y. P., and R. Leuning (1998), A two-leaf model for canopy conductance, photosynthesis and partitioning of available energy I: Model description and comparison with a multi-layered model, *Agric. For. Meteorol.*, *91*(1–2), 89–111, doi:10.1016/s0168-1923(98)00061-6.

Weng, E. S., and Y. Q. Luo (2008), Soil hydrological properties regulate grassland ecosystem responses to multifactor global change: A modeling analysis, *J. Geophys. Res.*, *113*, G03003, doi:10.1029/2007JG000539.

Williams, P. J., and M. W. Smith (1989), *The Frozen Earth Fundamentals of Geocryology*, Cambridge Univ. Press, Cambridge, U. K.

Xu, T., L. White, D. F. Hui, and Y. Q. Luo (2006), Probabilistic inversion of a terrestrial ecosystem model: Analysis of uncertainty in parameter estimation and model prediction, *Global Biogeochem. Cycles*, *20*, GB2007, doi:10.1029/2005GB002468.

Xu, X., Y. Q. Luo, and J. Z. Zhou (2012), Carbon quality and the temperature sensitivity of soil organic carbon decomposition in a tallgrass prairie, *Soil Biol. Biochem.*, *50*, 142–148, doi:10.1016/j.soilbio.2012.03.007.

Yi, Y., J. S. Kimball, M. A. Rawlins, M. Moghaddam, and E. S. Euskirchen (2015), The role of snow cover affecting boreal-arctic soil freeze-thaw and carbon dynamics, *Biogeosciences*, *12*(19), 5811–5829, doi:10.5194/bg-12-5811-2015.

Zhang, T. J. (2005), Influence of the seasonal snow cover on the ground thermal regime: An overview, *Rev. Geophys.*, *43*, RG4002, doi:10.1029/2004RG000157.

Zhang, Y., W. J. Chen, and J. Cihlar (2003), A process-based model for quantifying the impact of climate change on permafrost thermal regimes, *J. Geophys. Res.*, *108*(D22), 4695, doi:10.1029/2002JD003354

Zhang, Y., S. Wang, A. G. Baff, and T. A. Black (2008), Impact of snow cover on soil temperature and its simulation in a boreal aspen forest, *Cold Reg. Sci. Technol.*, *52*(3), 355–370, doi:10.1016/j.coldregions.2007.07.001.